Molecular Cell, Vol. 18, 49–60, April 1, 2005, Copyright ©2005 by Elsevier Inc. DOI 10.1016/j.molcel.2005.02.032

The Speed of RNA Transcription and Metabolite Binding Kinetics Operate an FMN Riboswitch

J. Kenneth Wickiser,[1,4] Wade C. Winkler,[2,5] Ronald R. Breaker,[2,*] and Donald M. Crothers[1,3,*]
[1]Department of Molecular Biophysics and Biochemistry
[2]Department of Molecular, Cellular and Developmental Biology
[3]Department of Chemistry
Yale University
New Haven, Connecticut 06520

Summary

Riboswitches are genetic control elements that usually reside in untranslated regions of messenger RNAs. These folded RNAs directly bind metabolites and undergo allosteric changes that modulate gene expression. A flavin mononucleotide (FMN)-dependent riboswitch from the *ribDEAHT* operon of *Bacillus subtilis* uses a transcription termination mechanism wherein formation of an RNA-FMN complex causes formation of an intrinsic terminator stem. We assessed the importance of RNA transcription speed and the kinetics of FMN binding to the nascent mRNA for riboswitch function. The riboswitch does not attain thermodynamic equilibrium with FMN before RNA polymerase needs to make a choice between continued transcription and transcription termination. Therefore, this riboswitch is kinetically driven, and functions more like a "molecular fuse." This reliance on the kinetics of ligand association and RNA polymerization speed might be common for riboswitches that utilize transcription termination mechanisms.

Introduction

A variety of distinct classes of riboswitches have been demonstrated to selectively bind target metabolites in the complete absence of protein factors (Winkler and Breaker, 2003; Mandal and Breaker, 2004; Nudler and Mironov, 2004; Vitreschak et al., 2004). Riboswitches are modular in architecture and are composed of two functional components: a ligand binding aptamer and an expression platform. Expression platforms of riboswitches make use of a variety of mechanisms for controlling gene expression, including the control of transcription termination, (e.g., Mironov et al., [2002], Winkler et al. [2002b], McDaniel et al. [2003], Sudarsan et al. [2003b], and Winkler et al. [2003]), and the control of translation initiation (e.g., Nahvi et al. [2002] and Vitreschak et al. [2002]). Because ~2% of the genes in *B. subtilis* are controlled by riboswitches, a detailed understanding of riboswitch function should aid in understanding how many essential metabolic genes are regulated.

In this study, we examine the mechanistic details of an FMN-responsive riboswitch from *B. subtilis*. This bacterium carries at least two FMN riboswitches (Mironov et al., 2002; Winkler et al., 2002a), wherein one (*ypaA*) controls translation initiation and the other (*ribD*) controls premature transcription termination. The *ribD* riboswitch variant resides within the 5′ UTR of the mRNA for the *ribDEAHT* operon, which encodes genes responsible for riboflavin biosynthesis. It has been proposed (Mironov et al., 2002; Winkler et al., 2002a) that the riboswitch operates by forming an intrinsic terminator stem (Wilson and von Hippel, 1995) when FMN is present in sufficient amounts but folds into an alternative structure when FMN is absent (Figure 1A).

The affinities that several classes of riboswitches exhibit for their target metabolites have been examined, and values reported for apparent dissociation constants (apparent K_D) range from ~5 nM for guanine (Mandal et al., 2003) and SAM (Winkler et al., 2003) riboswitches to ~200 μM for a glucosamine-6-phosphate riboswitch (Winkler et al., 2004). However, it is notable that the apparent K_D values for the aptamer domains from riboswitches do not necessarily correspond to the concentrations of metabolite needed to induce transcription termination in vitro (McDaniel et al., 2003; Sudarsan et al., 2003b; Winkler et al., 2003). This could be due to the presence of alternative structures formed by the RNA that interfere with metabolite binding as observed previously (Winkler et al., 2002a; Winkler et al., 2002b; Sudarsan et al., 2003b).

Some riboswitches could require higher concentrations of metabolite (relative to the K_D value), because riboswitch action might be dictated by the kinetics of ligand binding and by the speed at which RNA polymerase lengthens the nascent mRNA chain. Other examples of gene control in bacteria known to rely on polymerase speed include attenuation and T-box systems (Winkler and Yanofsky, 1981; Grundy and Henkin, 2004). Formation of an intrinsic terminator stem while the active site of RNA polymerase is positioned within the typical adjoining run of U residues leads to transcription termination (Reynolds and Chamberlin, 1992; Gusarov and Nudler, 1999; Yarnell and Roberts, 1999). However, if the *ribD* aptamer has not docked its target before RNA polymerase transcribes beyond the U-rich stretch (Figure 1A), it is proposed that the terminator stem is not formed, and transcription progresses and yields full-length mRNA. This mechanism might not provide sufficient time for the RNA-FMN interaction to reach thermodynamic equilibrium before RNA polymerase has passed the point in mRNA transcription where a decision is made whether or not to abort gene expression. If such kinetics are important, then concentrations of FMN higher than the apparent K_D value for the RNA-ligand complex would be needed to cause transcription termination. We set out to determine whether the FMN riboswitch from the *ribD* operon of

*Correspondence: ronald.breaker@yale.edu (R.R.B.); donald.crothers@yale.edu (D.M.C.)
[4]Present address: The Rockefeller University, 1230 York Avenue, Box 226, New York, New York 10021.
[5]Present address: Department of Biochemistry, University of Texas Southwestern Medical Center, Dallas, Texas 75390.

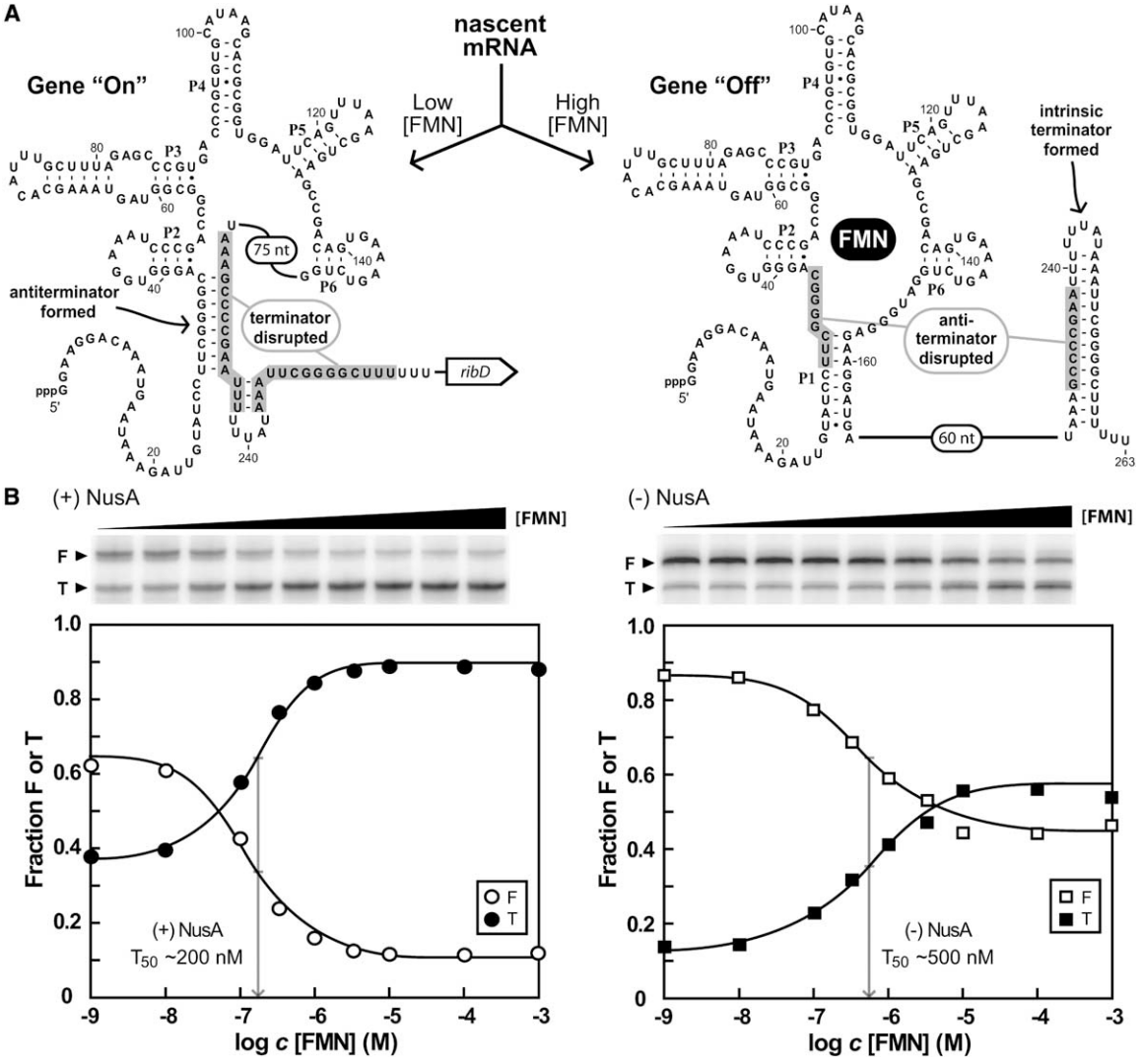

Figure 1. FMN Riboswitch from the *ribDEAHT* Operon of *B. subtilis*

(A) The FMN riboswitch employs a mechanism for gene control that relies on the mutually exclusive formation of intrinsic transcription terminator and antiterminator stem structures. At low FMN concentrations (left), nascent mRNA transcripts form the antiterminator stem and transcription of the entire mRNA proceeds. At high FMN concentrations (right), the aptamer forms a complex with FMN that prevents antiterminator formation, thus permitting formation of the terminator stem that halts extension of the mRNA. These two structural states do not necessarily interchange on a time scale that is relevant to the molecular events that control gene expression. Rather, each nascent mRNA likely commits to a riboswitch folding pathway that leads to the "Off" state or the "On" state, as dictated by the concentration of FMN, and then becomes kinetically trapped once either of the two folded structures has been adopted.

(B) Left: Top, autoradiogram of a denaturing 10% PAGE separation of products from a single-round transcription assay with a *ribD* template DNA, EcRNAP, 280 nM EcNusA, and 200 μM NTP. Products from each lane were generated during a transcription assay conducted for 20 min with concentrations of FMN ranging from 1 nM to 1 mM. See the Experimental Procedures for experimental details. Bottom, a plot of the fraction of full-length (F) or terminated (T) RNA products versus the concentration of FMN, where F + T = 1. Open and filled symbols represent full-length and terminated products, respectively. Right: Experiments are as described as above except that EcNusA was excluded from the assay.

B. subtilis is a kinetically driven or a thermodynamically driven riboswitch.

Results and Discussion

The Effect of FMN Concentration on Transcription Termination

The majority of riboswitches in gram-positive bacteria control gene expression through ligand-dependent competition between a properly folded aptamer structure and an alternate mutually exclusive structure that prohibits formation of a transcription termination signal. This mechanism can be examined in vitro by conducting transcription assays where levels of full-length and terminated RNA transcripts are established by using reaction mixtures containing different concentrations of ligand, as has been done previously for monitoring pausing of RNA polymerases during transcription due

Table 1. Effects of RNAP, NusA, and NTP Concentration on FMN-Mediated Transcription Termination of an FMN Riboswitch

Template	RNAP	NusA	(μM) [NTP]	F_L	F_H	T_L	T_H	CFT	(μM) T_{50}
Wt	Ec	–	200	0.86	0.46	0.14	0.54	0.40	0.48
Wt	Ec	Ec	200	0.62	0.12	0.38	0.88	0.50	0.16
Wt	Ec	Ec	500	0.54	0.21	0.46	0.79	0.33	0.34
Wt	Ec	Bs	200	0.85	0.34	0.15	0.66	0.51	0.17
Wt	Ec	Bs	500	0.82	0.50	0.18	0.50	0.32	0.32
Wt	Bs	–	200	0.58	0.42	0.42	0.58	0.16	1.86*
Wt	Bs	–	500	0.63	0.52	0.37	0.48	0.11	2.83*
Wt	Bs	Bs	200	0.60	0.34	0.40	0.66	0.26	2.33*
Wt	Bs	Bs	500	0.59	0.41	0.41	0.59	0.18	2.05*
PB	Ec	–	200	0.77	0.59	0.23	0.41	0.18	1.9*
PA/PB	Ec	–	200	0.70	0.57	0.30	0.43	0.13	1.9*
PA/PB	Bs	–	200	0.61	0.56	0.39	0.44	0.15	1.4*
PA/PB	Bs	Bs	200	0.54	0.44	0.46	0.56	0.10	2.2*

F represents the fraction of full-length transcript. T represents the fraction of terminated product. The subscripts L and H correspond to low (1 nM) and high (100 μM) concentrations of FMN. CFT (change in fraction terminated) is defined as $T_H - T_L$. T_{50} marks the FMN concentration required to give 50% of the termination response. Wt (wild-type) template is the natural 304 nucleotide leader of *ribD*, PB is the same template with the base substitutions at the second pause site, and PA/PB is the same template with base substitutions at both pause sites. Asterisks reflect T_{50} values generated from exceedingly small changes in FMN-mediated transcription termination (low CFT), and therefore the actual values for T_{50} might be even larger.

to either DNA-drug interactions (Phillips et al., 2001) or mRNA primary sequence and secondary structural contributions (Artsimovitch and Landick, 2000; Epshtein and Nudler, 2003; Gong and Yanofsky, 2003; Zhang and Switzer, 2003).

By using similar methods, we determined that a discrepancy also exists between the apparent K_D values for FMN binding to its corresponding riboswitch RNAs and the concentrations of FMN needed to trigger transcription termination (Figure 1B). Template DNAs carrying the natural promoter and 5′ UTR for the *ribD* operon from *B. subtilis* were transcribed by using RNA polymerase from *Esherichia coli* (EcRNAP) or from *B. subtilis* (BsRNAP) under conditions that synchronize transcription and that permit only a single transcription event to occur for each DNA template (see Experimental Procedures). Either EcRNAP or BsRNAP permits *ribD* riboswitch function, as revealed by changes in the levels of terminated and full-length RNAs when FMN is added to the reactions. (Table 1; see also Supplemental Data available online with this article).

Values were determined for a series of parameters, including the fraction of the transcripts that are full length (F) or terminated (T) at low or zero FMN concentration (F_L and T_L, respectively) or at high FMN concentrations (F_H and T_H, respectively). These parameters allow us to quantitatively describe the various effects of RNA polymerase type, FMN concentration, the effects of the protein transcription factor NusA (Farnham et al., 1982; Gusarov and Nudler, 2001), and ribonucleoside triphosphate (NTP) concentrations on riboswitch action. The FMN concentration required to cause a 50% change between T_H and T_L is defined as T_{50}. The FMN-mediated change in the fraction of terminated RNA transcripts (CFT) is defined as $T_H - T_L$. CFT can vary from zero, when there is no change in termination on FMN addition, to one, when all transcripts are full length in the absence of FMN and termination is 100% at high FMN concentration. The CFT value should become lower as the normal function of the riboswitch is made poorer by mutations or by altered conditions.

NusA is an RNA binding protein that is known to alter the levels of transcription termination when RNA polymerase transcribes other templates (Yakhnin and Babitzke, 2002; Carlomagno and Nappo, 2003). It has been demonstrated previously that NusA increases the time that RNA polymerase spends in paused states during transcription and that this perturbation in transcription kinetics affects nascent transcript folding (Pan et al., 1999). In the presence of NusA, FMN triggers increased transcription termination with a T_{50} of ~200 nM (Figure 1B, left), whereas the T_{50} for transcription termination in its absence is ~500 nM (Figure 1B, right). NusA also increases the fraction of terminated transcription products by ~2-fold both at low and at high FMN concentrations. Although the effects of NusA on T_{50} values are consistent with its effects on pause site lifetimes, we have not ruled out the possibility that NusA binding might alter the affinity that the riboswitch RNA exhibits toward FMN. Regardless, the T_{50} values measured in the presence of NusA are 30- to 100-fold higher than the 5 nM K_D value for the *ribD* aptamer when measured in isolation (Winkler et al., 2002a), although the two parameters were assessed under somewhat different reaction conditions.

The concentrations of NTPs used for transcription can similarly influence the extent of transcription termination mediated by riboswitches. Decreasing concentrations of NTPs have caused increased transcription termination for a glycine-specific riboswitch in a previous study (Mandal et al., 2004). A similar effect is observed with the FMN riboswitch (Table 1), wherein the use of 200 μM NTPs results in reduced levels of full-length transcript relative to the use of 500 μM NTPs. These findings are consistent with the hypothesis that slower speed of transcription will result in a greater level of termination because FMN has more time to bind to the riboswitch.

Mapping Transcriptional Intermediates

If a kinetic mechanism is involved, then the time needed for RNA polymerase to progress from the 3′

end of the aptamer to the intrinsic terminator should be an important parameter that influences the concentration of FMN needed to induce termination. The speed of RNA polymerase should be dependent on the speed of iterative rounds of nucleotide incorporation and translocation made by the polymerase and should also depend on transcriptional pausing, which can be caused by specific sequence elements in the DNA template (Artsimovitch and Landick, 2000).

To examine the possibility that transcriptional pausing is important for riboswitch function, we mapped the inherent pause sites that exist within the *ribD* leader sequence after the aptamer domain has been generated but before the transcriptional terminator is made (Figure 2A). Two prominent pause sites, PA and PB, near positions U215 and U245, respectively, of the *ribD* transcript were identified as incomplete transcripts. These products appear early during transcription but largely disappear as incubation times increase (Figure 2A). The termination site was verified to occur near position U263 in a previous study (Winkler et al., 2002a). For subsequent experiments, we defined paused RNAs at sites PA and PB as transcriptional intermediates whose lifetimes and FMN binding characteristics could play an integral role in the function of the *ribD* riboswitch.

Lifetimes of Pause Sites

The lifetimes of the paused complexes were estimated (see Experimental Procedures) by monitoring the appearance and disappearance of the PA and PB transcriptional intermediates. By using EcRNAP in a synchronized transcription assay containing 200 μM NTPs, PA had a lifetime of ~10 s, whereas PB had a lifetime of ~1 min (Figure 2B). The addition of either EcNusA or BsNusA increases the lifetimes of the pause sites, whereas increasing the concentration of NTPs decreases the pause lifetimes (data not shown), as expected given the respective influences these factors have on transcription speed. Preliminary results also indicate that BsRNAP pauses at the same sites as EcRNAP with lifetimes that are only slightly shorter (within 2-fold).

The Relationship between Pausing and Termination

To further investigate the role of transcriptional pausing in riboswitch function, we mutated the template at either or both PA and PB sites to ablate pausing. These mutant templates exhibit substantial decreases in pause site lifetimes (Figure S1). Mutating the nucleotides immediately upstream of PB (nucleotides 241–247 changed from UUUUAUA to ACACAUU) causes some degradation in the efficiency of riboswitch function, as reflected by a 2-fold drop in the CFT value relative to the wild-type (Table 1). In addition, a nearly 4-fold increase in the T_{50} value results. This is consistent with the hypothesis that the metabolite has less time for complex formation to occur with the nascent mRNA when pause sites are disrupted, thus leading to higher concentrations of FMN needed to trigger termination.

Likewise, the simultaneous alteration of sequences near PA (nucleotides 213–215 changed from UUG to ACA) coupled with the mutations at PB described above yield similar results to those observed when only a single pause site is disrupted. Specifically, the efficiency of riboswitch function is further reduced as reflected by even smaller CFT values, whereas the concentration of FMN needed to cause half-maximal termination remains high. Lower CFT values with pause mutants could be due to changes in the folding kinetics that can lead to increased misfolding and misfunction of riboswitch RNAs. The higher T_{50} values are consistent with the hypothesis that the overall time taken by the RNA polymerase to progress to the site of termination is important for establishing the FMN concentrations needed to trigger riboswitch function.

Binding of FMN by Transcriptional Intermediates

An alternative explanation for the higher T_{50} values is that ligand affinity might change as the length of the nascent RNA transcript increases, as has been observed previously (Winkler et al., 2002a; Sudarsan et al., 2003b; Winkler et al., 2003). Of particular concern are the transcriptional intermediates, as these RNAs are available for extended periods of time, and their nonaptamer regions might participate in alternative folding. The characteristics of the longest-lived intermediates were examined by creating RNA constructs that approximated the lengths of the nascent RNAs that protrude from RNA polymerase during transcription. The number of nucleotides at the growing 3′ end of the nascent RNA transcript that are encumbered by RNA polymerase (toeprint of BsRNAP) is ~12 nucleotides (Monforte et al., 1990; Komissarova and Kashlev, 1998). Therefore, we postulated that RNAs corresponding to ~200, 230, and 251 nucleotides would simulate the portions of the nascent RNAs that are free from RNA polymerase when paused at sites corresponding to PA, PB, and T, respectively (Figure 3A). The most obvious factor that could affect binding affinity is flanking sequences that form part of the antiterminator stem. These sequences are present in a construct termed 244 *ribD* that mimics the RNA-polymerase complex at the termination site (Figure 1A; nucleotides 1–244). A shorter RNA construct (165 *ribD*) that carries the entire aptamer domain was also prepared.

Apparent K_D values for RNAs representing these transcriptional intermediates were established by using in-line probing (Figure 3B) (Soukup and Breaker, 1999). From these patterns, it is estimated that 230 *ribD* RNA, the PB mimic, has an apparent K_D value (~100 nM) that is ~10-fold poorer than the value estimated for the 165 *ribD* construct (~10 nM). In contrast, the pattern of spontaneous cleavage products from 244 *ribD* RNA is not altered by FMN addition. Furthermore, there is a difference in the spontaneous cleavage pattern between 244 *ribD* and the shorter RNAs in the region spanning nucleotides 32–38. With the shorter RNAs, increasing FMN concentrations reduce spontaneous cleavage, as is expected because the conserved nucleotides in this region form part of the aptamer core (Winkler et al., 2002a). In contrast, this same region of 244 *ribD* exhibits reduced spontaneous cleavage regardless of the concentration of FMN, which is consistent with static formation of the antiterminator stem.

This suggests that the aptamer remains receptive to

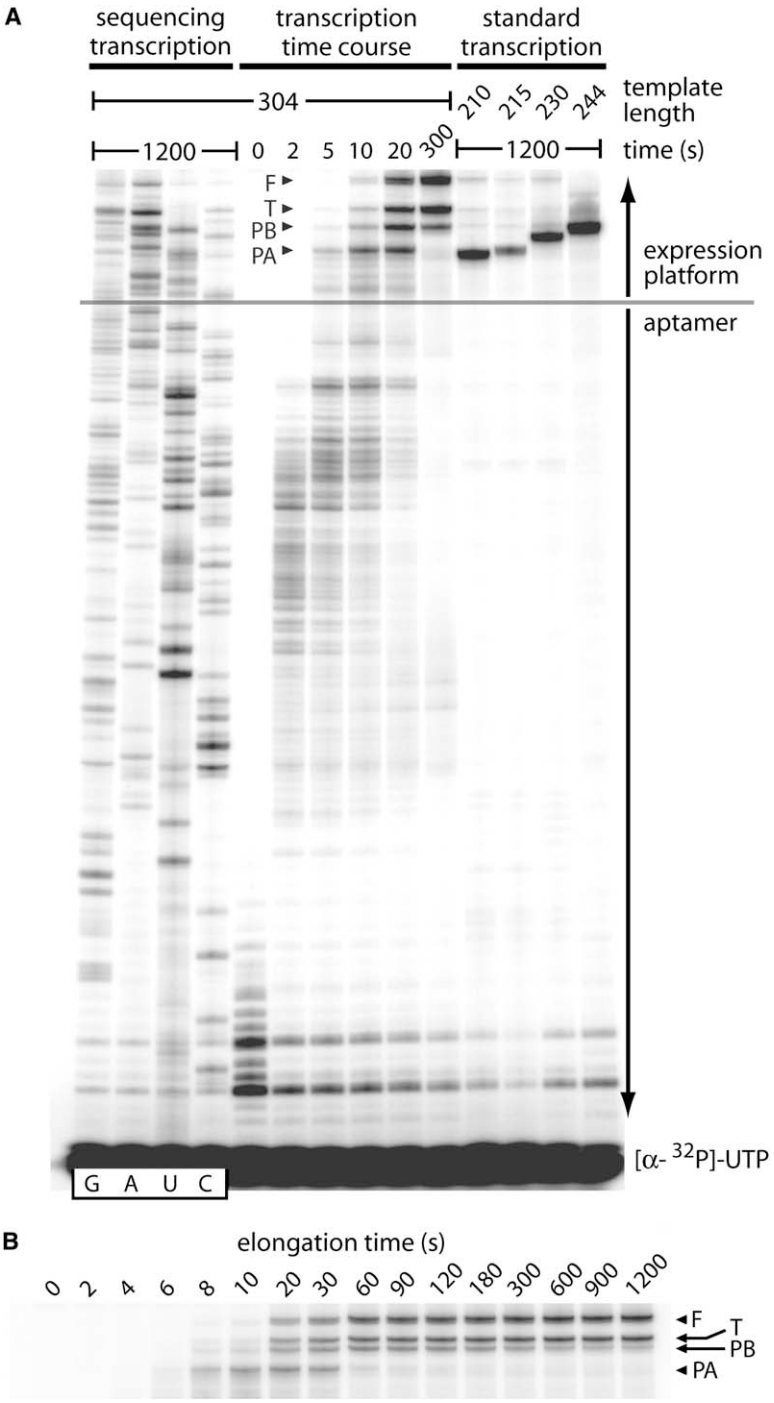

Figure 2. Identification of Transcriptional Intermediates

(A) Mapping of EcRNAP pause and termination sites with denaturing PAGE. Lanes labeled G, A, U, and C identify single-round transcription assays (see Experimental Procedures) conducted with 3′-O-Methyl-NTPs in the elongation mix by using the DNA template corresponding to the 304 nucleotide intergenic region upstream of the *B. subtilis ribD* operon. Similarly, a single-round transcription time course was conducted with normal NTPs to reveal the presence of transcriptional intermediates. RNA products in the right-most lanes were generated by transcribing (under standard run-off transcription conditions) DNA templates designed to yield RNA transcripts of the sizes indicated. F, T, PB, and PA indicate RNAs resulting when transcription proceeds to the template end (full length), to the termination site, to pause B, and to pause A, respectively.

(B) Establishing the lifetimes of pause sites by denaturing PAGE. Depicted is the portion of the gel carrying the RNA products from the 304 *ribD* DNA template when transcribed with EcRNAP using 200 μM NTP. Products are as described in (A).

FMN binding until it is disrupted by the formation of the antiterminator helix. This helix can only form when the right shoulder of the antiterminator (nucleotides 231–238) is generated. Furthermore, these findings are consistent with the hypothesis that the affinity of the aptamer domains of PA and PB have apparent K_D values that are better than those suggested by T_{50} values. Substantial loss of binding affinity occurs when the antiterminator stem forms in the 244 *ribD* construct, and this stem formation is likely to be the final and irreversible event in riboswitch function at low FMN concentrations. If the right shoulder of the antiterminator is formed by polymerase quickly, then there is insufficient time for the aptamer to attain binding equilibrium before antiterminator formation precludes FMN binding. Therefore, the critical determinants of *ribD* riboswitch function are most likely the rate constant for FMN association and the time required for polymerase to progress from the end of the aptamer to the termination site.

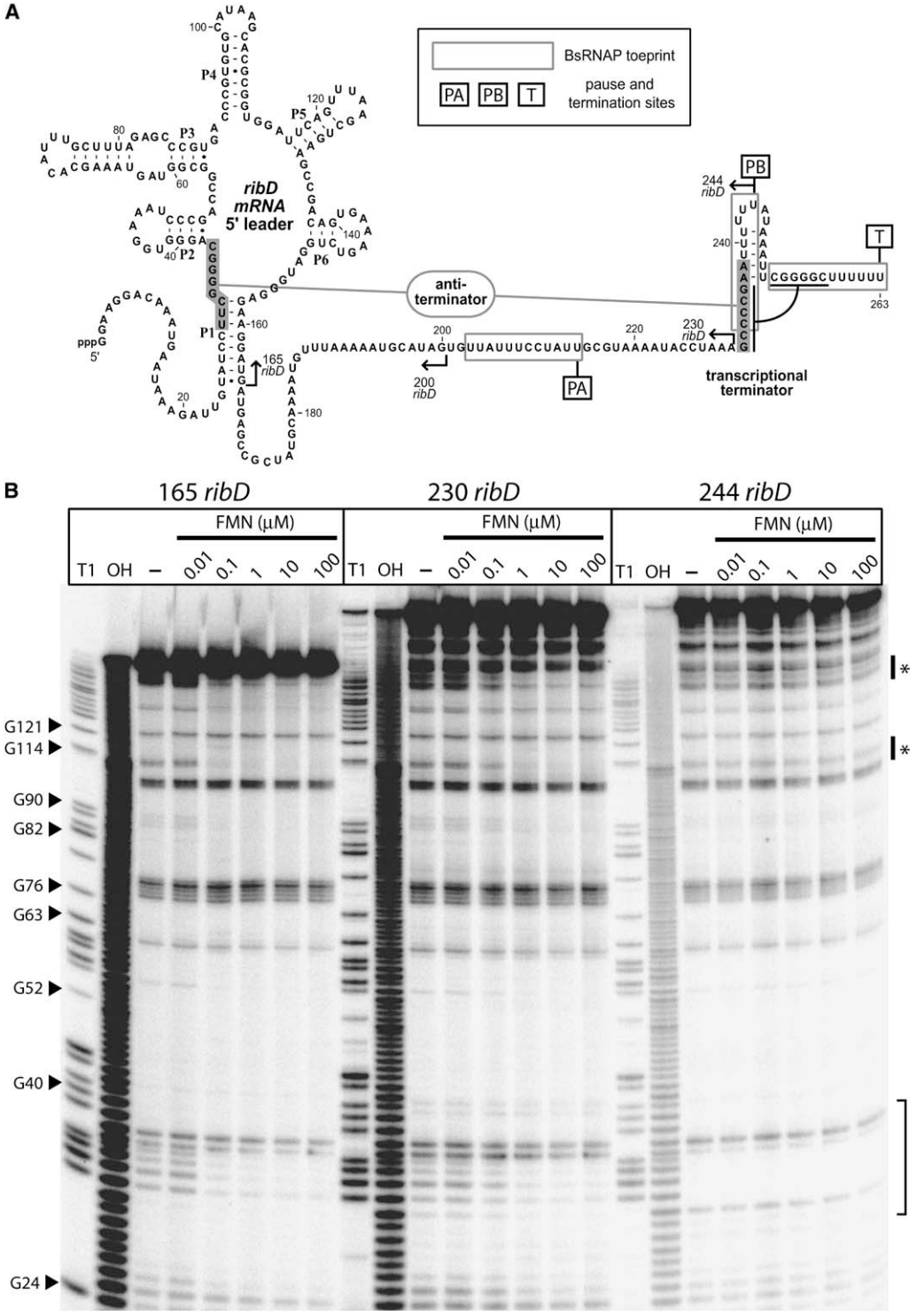

Figure 3. Transcriptional Intermediates and FMN Binding

(A) Sequence, secondary structure, and expected transcriptional intermediates of the 5′ UTR of the *ribD* mRNA from *B. subtilis*.

(B) In-line probing (see Experimental Procedures) results of three RNAs transcriptional intermediates of the *ribD* mRNA. Products of spontaneous RNA cleavage are separated by denaturing PAGE and visualized by PhosphorImager. T1 and OH lanes represent partial digestion with RNase T1 and alkali, respectively. RNAs were incubated at 25°C for 40 hr in the absence (–) of FMN and in the presence of various concentrations of FMN as indicated. Selected bands corresponding to RNase T1 cleavage 3′ of G residues are identified. Asterisks identify regions where substantial alteration of the pattern of spontaneous cleavage products occurs. The bracket identifies the region of the gel corresponding to cleavage that is indicative of FMN binding (165 *ribD* and 230 *ribD*) or antiterminator formation (244 *ribD*).

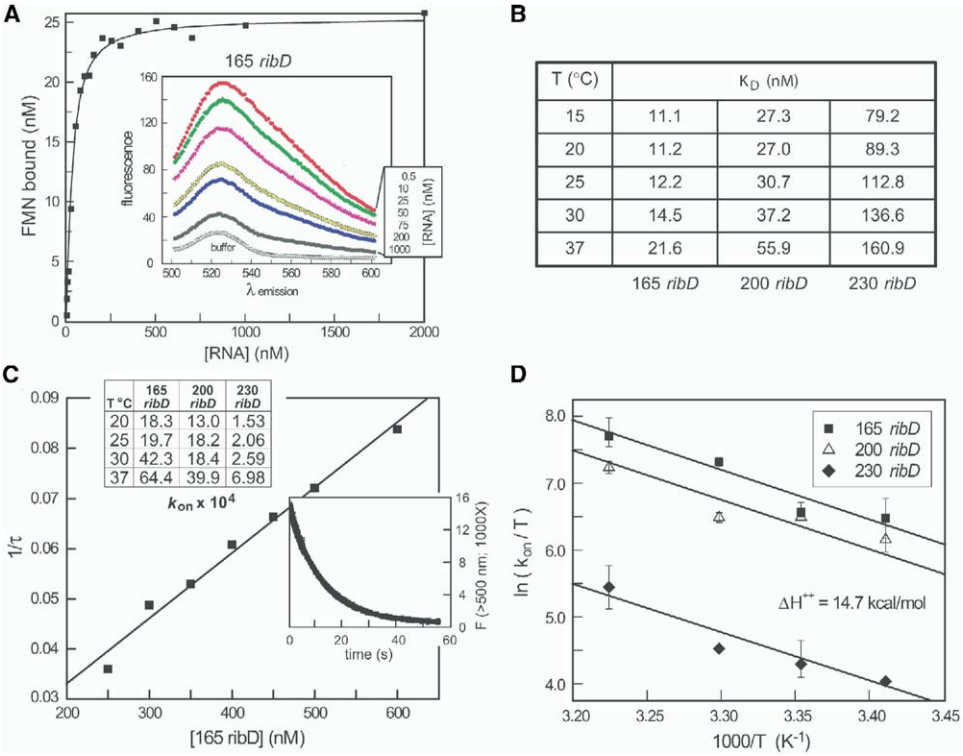

Figure 4. Analysis of FMN Binding to *ribD* RNAs by Monitoring Fluorescence Quenching

(A) FMN binding assay monitored by fluorescence quenching. Assays contained 25 nM FMN and 165 *ribD* and were incubated at 30°C. Data were fit to the K_D quadratic equation solution for 1:1 stoichiometry.

(B) K_D values measured by fluorescence quenching for various FMN riboswitch constructs.

(C) Determination of the k_{on} of FMN from a plot of the inverse time constant versus a range of final RNA concentrations. The slope of the plot yields the rate constant. The lower inset displays the fluorescence data that were fit to a single exponential formula to yield the plotted time constants. The process was repeated and averaged for each RNA at different temperatures. The upper inset table represents the average value of each determined rate constant.

(D) Eyring plot of the association rate constant for each RNA and FMN. The symbols represent the mean value of repetitions, and the error bars represent the range of values centered on the median. Note several error bars are smaller than the symbol.

Assessing Transcriptional Intermediates by Fluorescence

We also examined the equilibrium properties of the major transcriptional intermediates by using fluorescence methods. The strength of FMN binding can be established rapidly by monitoring quenching of the intrinsic fluorescence of FMN upon forming a complex with RNA (Mironov et al., 2002). For example, the robust fluorescence signal observed near 520 nm becomes progressively quenched as increasing concentrations of 165 *ribD* RNA are added (Figure 4A). Similar data were collected with the longer RNA transcripts 200 *ribD* (PA mimic) and 230 *ribD* (PB mimic) to generate a series of K_D values for each of these RNAs at various temperatures (Figure 4B).

The K_D value of 11 nM for 165 *ribD* obtained from FMN fluorescence quenching experiments at 25°C closely approximates the value estimated from in-line probing studies (Figure 3B) and the value reported previously (Winkler et al., 2002a). The K_D for the longest RNA examined (230 *ribD*) is still more than an order of magnitude better than the T_{50} observed with BsRNAP (Table 1). Therefore, the disparity between the K_D values for FMN binding and the concentration of this ligand needed to achieve 50% transcription termination indicates that the *ribD* riboswitch is likely to be kinetically controlled. Additional fluorescence experiments are consistent with this mechanism (Figures S3 and S4).

Ligand Binding Kinetics of an FMN Aptamer

We speculated that the specific rate constants for FMN association with the *ribD* riboswitch might be the key factor in establishing the T_{50} for this riboswitch. Therefore, we sought to directly measure the rate constants for FMN association (k_{on}) and dissociation (k_{off}) with the relevant transcriptional intermediates. By using a stopped-flow fluorimeter, the rate constant for FMN binding to *ribD* RNAs was measured under pseudofirst order conditions (RNA in large excess over FMN). The data fit a first-order exponential equation (see lower inset, Figure 4C), and the inverse of the resulting time constant (the time required for e^{-1} of the reaction to go toward completion) was plotted against the final concentration of RNA (Figure 4C). The resulting k_{on} value for FMN binding to 165 *ribD*, $\sim 10^5$ $M^{-1}s^{-1}$, falls within the spectrum of FMN binding to various flavoproteins (Haines et al., 2000). Whereas the k_{on} value for 200 *ribD* was similar to 165 *ribD*, the k_{on} value for 230 *ribD* was

approximately 10-fold poorer at all temperatures examined (see upper inset, Figure 4C).

If FMN is present in excess over the target mRNA, as must be the case for FMN regulation to be effective, a solution containing 1 μM of FMN would yield an association reaction time constant for 200 *ribD* of ~8 s and ~65 s for 230 *ribD* at 20°C. Similarly, at 37°C, it would take only 2 s and 34 s, respectively, for about half of the 200 *ribD* and 230 *ribD* RNA molecules to bind FMN. Furthermore, by increasing the concentration of FMN, the time constant would decrease accordingly.

These rate constants for the binding of FMN to *ribD* RNAs give relevance to the lengthy transcriptional pause lifetimes. A substantial amount of transcribing RNAP reaches the first pause site within 6 s after the start of transcription elongation, whereas the majority of RNAs have been synthesized beyond both pause sites and reach the transcription termination site after approximately 60 s has elapsed (Figure 2B). Thus, if the pause sites did not exist, far greater than 1 μM FMN would be needed to bind the riboswitch with sufficient speed.

A study of the temperature dependence of k_{on} indicates that the activation energy barrier of FMN binding for each RNA is approximately equal (Figure 4D). We conclude that, although the mechanism of ligand binding is likely the same for each RNA, the difference in rate constants for ligand association between the 200 *ribD* and the 230 *ribD* RNAs is most likely due to sampling of alternate folds caused by the presence of additional nucleotides in the longer RNA (see also Figure S3).

Lifetime of the RNA-FMN Complex

To gain insight into the lifetime of FMN-RNA complexes during transcription, we performed in vitro transcription assays with the *ribD* leader DNA template while monitoring the quenching of FMN fluorescence (Figure 5A). The status of FMN-RNA complexes was observed by adding heparin to transcription reactions at various times to inhibit further transcription initiation, after which point the fluorescence remains essentially unchanged. These data suggest that the FMN is only slowly released from the transcripts or that FMN redocks to the RNA if the ligand is released.

Rate constants for FMN dissociation from the *ribD* aptamer were examined by using a dilution-relaxation method employing a stopped-flow fluorimeter. The smaller transcriptional intermediate represented by the 200 *ribD* RNA construct was preequilibrated with FMN and then diluted with buffer to cause the complex to reach a new binding equilibrium, which results in a gain of fluorescence as FMN dissociates from the RNA (Figure 5B). The recovery from the initial to final equilibrium values follows a single exponential curve, wherein the time constant reflects a combination of the k_{on} and k_{off} values. The time constants, although temperature dependent, still must involve values for k_{off} that are so poor that equilibrium is likely never able to be achieved in the cell.

For example, at 25°C, the k_{off} value for 165 *ribD* is on the order of 10^{-3} s^{-1}, which translates to a time constant of approximately 10 min. In order to achieve equilibrium, the reaction would likely have to proceed for a much longer time when FMN concentrations are below the K_D. Given the typical half-lives of mRNAs within bacterial cells (Selinger et al., 2003), it is unlikely that equilibrium is achieved, and therefore a riboswitch with these characteristics must be kinetically, rather than thermodynamically, controlled. Our results, which indicate even slower dissociation for other transcription intermediates, are not consistent with data reported previously (Mironov et al., 2002) that supported a model for this riboswitch wherein multiple alternate binding-incompetent and thermodynamically stable RNA conformations form to ensure "recycling" of FMN after transcriptional termination.

Kinetics of Antiterminator Helix Formation

Another key aspect of the kinetic model for the *ribD* riboswitch is the necessity for the antiterminator helix to form (when FMN has not bound to the aptamer) between the time of accessibility of its right shoulder and the synthesis and exposure of sufficient nucleotides that permit formation of the terminator helix (Figure 3A). The polymerase must incorporate ~20 nucleotides to progress from PB to the site of transcription termination. If the polymerase elongated the RNA in this region at a rate of ~25 nucleotides per second (Rhodes and Chamberlin, 1974), then the right shoulder of the antiterminator strand would have about one second to anneal to its complement and prevent termination. Should the time from the end of PB until the point of termination be shorter than the time required for antiterminator helix formation, the latter could not form, and the riboswitch would default to terminate transcription regardless of whether FMN was bound.

In order to estimate the rate of formation of the antiterminator helix, we first used competition kinetics to measure the rate of bimolecular reaction of 230 *ribD* with an 8-mer antiterminator oligonucleotide (ATO) corresponding to the right shoulder of the antiterminator helix (Figure 5C). A 10-fold excess of ATO over FMN was required to reduce the FMN reaction rate by half, implying a 10-fold slower rate constant than for FMN, yielding a value of about 10^3 $M^{-1}s^{-1}$ for the ATO association rate constant (Figure 5D). Thus, accessibility or energetic factors cause the rate to be at least 100 times slower than typical nucleic acid hybridization rates. We next assume that this same factor applies to intramolecular loop closure and use the rate for closing a similar sized loop in the last step of tRNA unfolding (Crothers et al., 1974) as a value typical for an unencumbered intramolecular hybridization reaction. Reducing that rate by 100-fold yields at least 3 s as the time needed for intramolecular antiterminator helix formation, which is close to the time we estimate to be available during polymerase progression from PB to the termination site. The results further verify that FMN and the ATO bind competitively and that the ATO does not accelerate FMN dissociation (see also Figure S5).

The dissociation times of both FMN and the ATO are very long compared to the polymerase transit time from PB to the termination point. Therefore, this kinetically controlled riboswitch is better described as a molecular fuse. Once the riboswitch has committed to a particular state (FMN bound or antiterminator formed), the time needed to reverse this state is far longer than the time needed for the polymerase to pass the point in the tem-

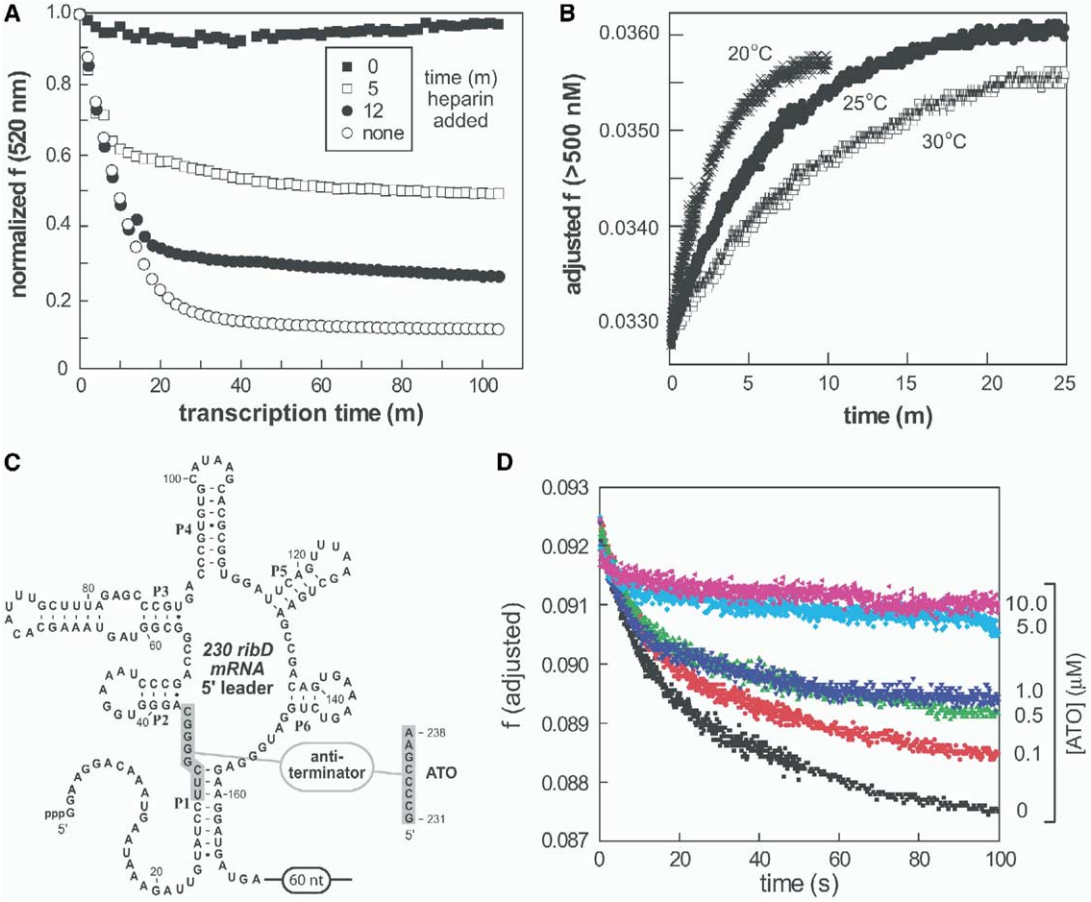

Figure 5. Establishing the Duration of the RNA-FMN Complex during Transcription and Competition between FMN Binding and Antiterminator Stem Formation

(A) Monitoring FMN fluorescence (f) quenching during transcription of *ribD* RNA. Transcriptions were carried out with EcRNAP at 37°C under conditions where multiple transcription initiation events are permitted on each DNA template. However, heparin is added in excess at the times noted to prevent further transcription initiation.

(B) Plot of the unquenching of FMN fluorescence (f) due to dissociation of FMN from the aptamer when a dilution-relaxation experiment is conducted with a 100 nM complex of FMN and 200 *ribD* RNA at the temperature indicated.

(C) Sequences and secondary structure model for the interaction between 230 *ribD* RNA and a DNA antiterminator oligonucleotide (ATO). The ATO corresponds to the *ribD* riboswitch sequence (Figure 3A) spanning nucleotides 231–238.

(D) Quenching of FMN fluorescence (f) in the presence of various concentrations of ATO by 230 *ribD*. F values for each sample were adjusted and scaled to yield a plot wherein F values at time zero are identical. Final reaction solutions were formed by combining 150 nM 230 *ribD* RNA with a mixture of 150 nM FMN and increasing amounts of ATO DNA. Each mixture also contained 50 mM MOPS (pH 7.5 at 25°C), 100 mM KCl, and 2 mM $MgCl_2$ and were incubated at 25°C.

plate where a decision regarding gene expression will be made. However, leakiness seems to be evident in this mechanism based on our in vitro transcription assays, which might even be a preferred characteristic for certain genetic switches.

Conclusions

There are now several examples of riboswitches that exhibit disparity between K_D values for metabolite binding and the concentrations of metabolite needed to half-maximally trigger transcription termination. These differences could be due, at least in part, to variations in the K_D values that are exhibited by transcription intermediates that carry different-length sequences at their growing 3′ ends. Another possibility is that metabolite binding affinities could be influenced by contacts between riboswitch RNAs and RNA polymerase or NusA that might be successively made and broken as transcription progresses along the DNA template.

Our findings, however, are consistent with a model wherein the speed of RNA polymerase causes it to reach the transcription termination point in the template long before the riboswitch attains a state of thermodynamic equilibrium for the aptamer-ligand interaction. We conclude that the *ribD* riboswitch and most likely several other classes of riboswitches with similar properties are kinetically driven genetic switches that are triggered only when concentrations of metabolite are substantially higher than the K_D values determined for their aptamer domains. A corollary is that one cannot estimate the concentrations of metabolite in vivo by establishing the apparent K_D values for riboswitch-metabolite complexes. The complicated depen-

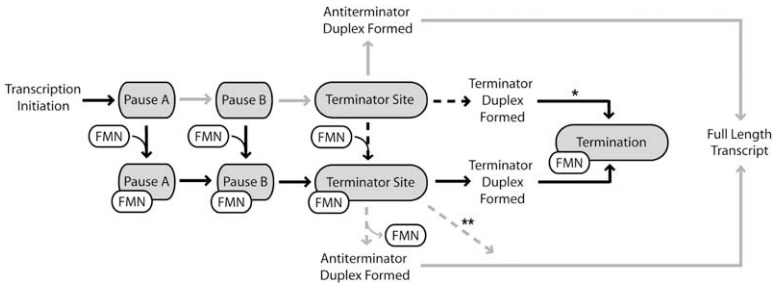

Figure 6. A Kinetic Model of the Mechanism for Transcription Control by an FMN Riboswitch

Paths depicted with black arrows lead to transcription termination, whereas the paths depicted with gray arrows lead to the production of full-length transcripts. Solid lines represent likely or fast transitions, whereas the dashed lines indicate slow or unlikely conversions. Dissociation of FMN does not impact the mechanism because it is likely to occur on a timescale that is far too large compared to the time required for the riboswitch to complete its function. The path identified with a single asterisk could produce some terminated transcripts that are not bound to FMN, whereas the path identified with two asterisks could produce full-length RNAs that are bound to FMN. Gray shading identifies RNA transcription intermediates. The kinetic parameters established in this study are related to this model in Figure S6.

dence of T_{50} on polymerase kinetics makes hazardous any extrapolation from an in vitro assay to in vivo conditions.

A pathway for the function of the *ribD* riboswitch is modeled in Figure 6. The model is consistent with the kinetic parameters that were measured in this study and highlights the hypothesis that FMN binding occurs primarily while RNA polymerase is paused. The model depicts two of the likeliest pathways (solid lines) for riboswitch function, wherein FMN binding favors formation of an intrinsic terminator stem and the absence of FMN leads to the production of full-length RNA. This choice in folding pathway occurs because FMN binding is predicted to sequester nucleotides (in part by formation of the P1 stem) that otherwise would form an antiterminator structure. Thus, FMN binding permits formation of the intrinsic terminator and transcription is aborted (Figure 1).

It is important to note that this kinetic framework is simplified and that numerous off-pathway molecular species probably contribute to the CFT and T_{50} values measured in this study. For example, the fact that we measured CFT values of no greater than 0.5 (Table 1) indicates that at least half the riboswitches produced by transcription in vitro were not functioning as predicted by the main paths depicted in our model. However, the lifetime of the transcriptional intermediates produced when polymerase pauses at sites PA and PB (Figure 2) are far shorter than the lifetimes of individual RNA-FMN complexes (Figures 4 and 5). Once a riboswitch RNA is bound to FMN, it is unlikely to release this ligand during the brief time needed for the polymerase to reach the site of intrinsic termination. Thus, there is not sufficient time for the riboswitch to approach equilibrium, which requires that there be enough time for several cycles of binding and dissociation to take place.

Given the complexity of transcription elongation, metabolite binding, RNA folding, and transcription termination processes, we believe that further experiments are needed to more precisely define the mechanistic details of riboswitches. However, our survey of these features leads us to postulate that many other riboswitches with a disparity between the K_D and T_{50} values will be governed by kinetic, rather than thermodynamic, parameters of metabolite binding. A key feature of control by kinetic competition is coupling of the regulatory "set point," or T_{50} value, to the rate of RNA synthesis. Longer pause lifetimes imply a lower T_{50}, down to the limit set by the thermodynamic K_D. Thus, this and other normally kinetically driven riboswitches might have thermodynamic character given unusual cellular conditions such as low NTP concentration. Such kinetically driven processes might also be present in riboswitches that use other mechanisms for gene control, such as RNA splicing (Kubodera et al., 2003; Sudarsan et al., 2003a). Moreover, other riboswitches exist that appear to exploit self-cleaving ribozyme (Winkler et al., 2004) or antisense (Rodionov et al., 2004) strategies that also could encompass elements of kinetic-driven processes. The overall complexity and diversity of riboswitch mechanisms are well suited for controlling genes in modern organisms. Similarly, such sophisticated RNAs could have performed complex molecular sensing and control functions in ancient RNA world organisms long before proteins had emerged in evolution.

Experimental Procedures

Chemicals and Oligonucleotides

Details regarding sources and processing of chemicals and oligonucleotides are described in the Supplemental Data.

In Vitro Transcription Termination and Pause Site Studies

Synchronized transcription reactions were conducted by using a protocol modified from those described previously (Landick et al., 1996; Phillips et al., 2001). Details for the reaction constituents and experimental procedures used to prepare BsRNAP and BsNusA are described in the Supplemental Data.

Estimation of Pause Lifetimes

Lifetimes of the paused complexes PA and PB were estimated by plotting the intensity of the radioisotope signals in polyacrylamide gel electrophoresis (PAGE) product bands. For each pause site, the temporal window corresponding to half-maximal occupation was defined as the lifetime of the intermediate.

Ligand Binding Kinetics

Stopped-flow experiments were conducted on an Applied Photophysics SX-18 apparatus. The fluorescence signal was generated by excitation at 445 nm using 1 mm slit widths and monitored above 500 nm by using a long pass-colored glass filter. Data were collected for approximately four times the time constant. Binding experiments were carried out in reaction buffer (RB) containing 50 mM MOPS (pH 7.5 at 25°C), 100 mM KCl, and 2 mM $MgCl_2$. All samples were stored on ice and incubated at the appropriate temperature for ~10 min prior to use. Photobleaching of FMN was determined to be an insignificant contribution to the signal change.

Rate Constants

Rate constants for FMN association with RNA (k_{on}) were determined by mixing equal volumes of solutions containing RNA and FMN in RB. For experiments wherein the RNA concentration was far greater than that of FMN, the time constants from the traces of each sample were averaged, inverted, and then plotted against final RNA concentration to attain the second order rate constant as described in the Supplemental Data. The k_{on} measurements were repeated several times at each temperature, and the average is depicted in Figure 4D. The range of k_{on} values was calculated, and the median was plotted as a bar ±0.5 range.

The rate constants for FMN dissociation from RNA (k_{off}) were determined by using the stopped-flow apparatus via dilution relaxation. The RNA-FMN complex in RB was diluted with an equivalent volume of RB, and the fluorescence signal increase was monitored over time. Given the known values for k_{on}, the reagent concentrations, and the K_D, a kinetic simulation was performed to estimate k_{off} (Supplemental Data).

K_D Values

FMN was held constant at either 25 nM (for 165 and 200 *ribD*) or 50 nM (for 230 *ribD*), and the fluorescence was measured while varying RNA concentration. The RNA-FMN samples were held on ice, degassed by bubbling helium, transferred to a quartz cuvette, and placed in the multicell peltier block of a Cary Eclipse fluorimeter and held at 15°C. Emission scans were performed from 500–600 nm (exciting at 445 nm) at 15, 20, 25, 30, and 37°C while waiting 7 min between each temperature change to allow for reequilibration of the FMN-RNA complex. See the Supplemental Data for further details.

Fluorescence Quenching during RNA Transcription

RNA transcription assays were conducted by using EcRNAP (Epicentre) that was combined with a solution containing buffer, NTPs, FMN, and DNA template to start the reaction. The transcription buffer was comprised of 4 mM $MgCl_2$, 37.5 mM KCl, 12 mM Tris-HCl (pH 7.5 at 25°C), and 0.01% Triton X-100. The transcription reaction solution included 100 μM NTPs, 100 nM FMN, and 50 pmoles of DNA template. To initiate the reaction, 45 picomoles of polymerase were added for a final reaction volume of 200 μL. Each solution was degassed by using helium and heated to 37°C prior to initiating the reaction. At the appropriate time, 2 μl of 10 mg mL^{-1} heparin was added to the reaction. Data were collected as described above and in the Supplemental Data. The multicell peltier block was maintained at 37°C, and the data were normalized to the time zero fluorescence reading.

FMN and ATO Competition Studies

Kinetic competition between ATO (5′-GCCCCGAA-3′) and FMN was conducted by using 200 *ribD* (data not shown) or 230 *ribD* RNA in RB that was mixed with a solution of FMN and increasing amounts of antiterminator strand DNA (ATO). A DNA ATO was used in order to utilize an RNase H assay (NEB), which provided confidence that oligonucleotide binding was occurring at the intended site only (data not shown).

Supplemental Data

Supplemental Data include Supplemental Results and Discussion, Supplemental Experimental Procedures, Supplemental References, and six figures and are available with this article online at http://www.molecule.org/cgi/content/full/18/1/49/DC1/.

Acknowledgments

We thank C. Conant and P. von Hippel for the kind gift of *E. coli* NusA protein and helpful discussions regarding its use. We appreciate the work of Dr. Mark Fisher of Varian Inc. for writing temperature-ramping software for the Cary Eclipse fluorimeter. We also thank M. Hulett for the generous gift of the *B. subtilis* strain MH5636 that produces oligohistidine-tagged BsRNAP and P. Babitzke for the generous gift of *E. coli* strain M15[pREP4] that produces oligohistidine-tagged BsNusA. This work was supported by National Institutes of Health (NIH) (GM068819) and National Science Foundation (EIA-0323510) grants to R.R.B. and by NIH grant GM 21966 and National Foundation for Cancer Research support to D.M.C.

Received: December 15, 2004
Revised: January 28, 2005
Accepted: February 22, 2005
Published: March 31, 2005

References

Artsimovitch, I., and Landick, R. (2000). Pausing by bacterial RNA polymerase is mediated by mechanistically distinct classes of signals. Proc. Natl. Acad. Sci. USA *97*, 7090–7095.

Carlomagno, M.S., and Nappo, A. (2003). NusA modulates intragenic termination by different pathways. Gene *308*, 115–128.

Crothers, D.M., Cole, P.E., Hilbers, C.W., and Shulman, R.G. (1974). The molecular mechanism of thermal unfolding of *Escherichia coli* formylmethionine transfer RNA. J. Mol. Biol. *87*, 63–88.

Epshtein, V., and Nudler, E. (2003). Cooperation between RNA polymerase molecules in transcription elongation. Science *300*, 801–805.

Farnham, P.J., Greenblatt, J., and Platt, T. (1982). Effects of NusA protein on transcription termination in the tryptophan operon of *Escherichia coli*. Cell *29*, 945–951.

Gong, F., and Yanofsky, C. (2003). A transcriptional pause synchronizes translation with transcription in the tryptophanase operon leader region. J. Bacteriol. *185*, 6472–6476.

Grundy, F.J., and Henkin, T.M. (2004). Kinetic analysis of tRNA-directed transcription antitermination of the *Bacillus subtilis* glyQS gene *in vitro*. J. Bacteriol. *186*, 5392–5399.

Gusarov, I., and Nudler, E. (1999). The mechanism of intrinsic transcription termination. Mol. Cell *3*, 495–504.

Gusarov, I., and Nudler, E. (2001). Control of intrinsic transcription termination by N and NusA: the basic mechanisms. Cell *107*, 437–449.

Haines, D.C., Sevrioukova, I.F., and Peterson, J.A. (2000). The FMN-binding domain of cytochrome P450BM-3: resolution, reconstitution, and flavin analogue substitution. Biochemistry *39*, 9419–9429.

Komissarova, N., and Kashlev, M. (1998). Functional topography of nascent RNA in elongation intermediates of RNA polymerase. Proc. Natl. Acad. Sci. USA *95*, 14699–14704.

Kubodera, T., Watanabe, M., Yoshiuchi, K., Yamashita, N., Nishimura, A., Nakai, S., Gomi, K., and Hanamoto, H. (2003). Thiamine-regulated gene expression of *Aspergillus oryzae* thiA requires splicing of the intron containing a riboswitch-like domain in the 5′-UTR. FEBS Lett. *555*, 516–520.

Landick, R., Wang, D., and Chan, C.L. (1996). Quantitative analysis of transcriptional pausing by *Escherichia coli* RNA polymerase: his leader pause site as paradigm. Methods Enzymol. *274*, 334–353.

Mandal, M., and Breaker, R.R. (2004). Gene regulation by riboswitches. Nat. Rev. Mol. Cell Biol. *5*, 451–463.

Mandal, M., Boese, B., Barrick, J.E., Winkler, W.C., and Breaker, R.R. (2003). Riboswitches control fundamental biochemical pathways in *Bacillus subtilis* and other bacteria. Cell *113*, 577–586.

Mandal, M., Lee, M., Barrick, J.E., Weinberg, Z., Emilsson, G.M., Ruzzo, W.L., and Breaker, R.R. (2004). A glycine-dependent riboswitch that uses cooperative binding to control gene expression. Science *306*, 275–279.

McDaniel, B.A., Grundy, F.J., Artsimovitch, I., and Henkin, T.M. (2003). Transcription termination control of the S box system: direct measurement of *S*-adenosylmethionine by the leader RNA. Proc. Natl. Acad. Sci. USA *100*, 3083–3088.

Mironov, A.S., Gusarov, I., Rafikov, R., Lopez, L.E., Shatalin, K., Kreneva, R.A., Perumov, D.A., and Nudler, E. (2002). Sensing small molecules by nascent RNA: a mechanism to control transcription in bacteria. Cell *111*, 747–756.

Monforte, J.A., Kahn, J.D., and Hearst, J.E. (1990). RNA folding during transcription by *Escherichia coli* RNA polymerase analyzed by RNA self-cleavage. Biochemistry *29*, 7882–7890.

Nahvi, A., Sudarsan, N., Ebert, M.S., Zou, X., Brown, K.L., and Breaker, R.R. (2002). Genetic control by a metabolite binding mRNA. Chem. Biol. *9*, 1043.

Nudler, E., and Mironov, A.S. (2004). The riboswitch control of bacterial metabolism. Trends Biochem. Sci. *29*, 11–17.

Pan, T., Artsimovitch, I., Fang, X.W., Landick, R., and Sosnick, T.R. (1999). Folding of a large ribozyme during transcription and the effect of the elongation factor NusA. Proc. Natl. Acad. Sci. USA *96*, 9545–9550.

Phillips, D.R., Cutts, S.M., Cullinane, C.M., and Crothers, D.M. (2001). High-resolution transcription assay for probing drug-DNA interactions at individual drug sites. Methods Enzymol. *340*, 466–485.

Reynolds, R., and Chamberlin, M.J. (1992). Parameters affecting transcription termination by *Escherichia coli* RNA. II. Construction and analysis of hybrid terminators. J. Mol. Biol. *224*, 53–63.

Rhodes, G., and Chamberlin, M.J. (1974). Ribonucleic acid chain elongation by *Escherichia coli* ribonucleic acid polymerase. I. Isolation of ternary complexes and the kinetics of elongation. J. Biol. Chem. *249*, 6675–6683.

Rodionov, D.A., Vitreschak, A.G., Mironov, A.A., and Gelfand, M.S. (2004). Comparative genomics of the methionine metabolism in Gram-positive bacteria: a variety of regulatory systems. Nucleic Acids Res. *32*, 3340–3353.

Selinger, D.W., Saxena, R.M., Cheung, K.J., Church, G.M., and Rosenow, C. (2003). Global RNA half-life analysis in *Escherichia coli* reveals positional patterns of transcript degradation. Genome Res. *13*, 216–223.

Soukup, G.A., and Breaker, R.R. (1999). Relationship between internucleotide linkage geometry and the stability of RNA. RNA *5*, 1308–1325.

Sudarsan, N., Barrick, J.E., and Breaker, R.R. (2003a). Metabolite-binding RNA domains are present in the genes of eukaryotes. RNA *9*, 644–647.

Sudarsan, N., Wickiser, J.K., Nakamura, S., Ebert, M.S., and Breaker, R.R. (2003b). An mRNA structure in bacteria that controls gene expression by binding lysine. Genes Dev. *17*, 2688–2697.

Vitreschak, A.G., Rodionov, D.A., Mironov, A.A., and Gelfand, M.S. (2002). Regulation of riboflavin biosynthesis and transport genes in bacteria by transcriptional and translational attenuation. Nucleic Acids Res. *30*, 3141–3151.

Vitreschak, A.G., Rodionov, D.A., Mironov, A.A., and Gelfand, M.S. (2004). Riboswitches: the oldest mechanism for the regulation of gene expression? Trends Genet. *20*, 44–50.

Wilson, K.S., and von Hippel, P.H. (1995). Transcription termination at intrinsic terminators: the role of the RNA hairpin. Proc. Natl. Acad. Sci. USA *92*, 8793–8797.

Winkler, M.E., and Yanofsky, C. (1981). Pausing of RNA polymerase during in vitro transcription of the tryptophan operon leader region. Biochemistry *20*, 3738–3744.

Winkler, W.C., and Breaker, R.R. (2003). Genetic control by metabolite-binding riboswitches. ChemBioChem *4*, 1024–1032.

Winkler, W.C., Cohen-Chalamish, S., and Breaker, R.R. (2002a). An mRNA structure that controls gene expression by binding FMN. Proc. Natl. Acad. Sci. USA *99*, 15908–15913.

Winkler, W.C., Nahvi, A., and Breaker, R.R. (2002b). Thiamine derivatives bind messenger RNAs directly to regulate bacterial gene expression. Nature *419*, 952–956.

Winkler, W.C., Nahvi, A., Sudarsan, N., Barrick, J.E., and Breaker, R.R. (2003). An mRNA structure that controls gene expression by binding *S*-adenosylmethionine. Nat. Struct. Biol. *10*, 701–707.

Winkler, W.C., Nahvi, A., Roth, A., Collins, J.A., and Breaker, R.R. (2004). Control of gene expression by a natural metabolite-responsive ribozyme. Nature *428*, 281–286.

Yakhnin, A.V., and Babitzke, P. (2002). NusA-stimulated RNA polymerase pausing and termination participates in the *Bacillus subtilis* trp operon attenuation mechanism *in vitro*. Proc. Natl. Acad. Sci. USA *99*, 11067–11072.

Yarnell, W.S., and Roberts, J.W. (1999). Mechanism of intrinsic transcription termination and antitermination. Science *284*, 611–615.

Zhang, H., and Switzer, R.L. (2003). Transcriptional pausing in the *Bacillus subtilis pyr* operon *in vitro*: a role in transcriptional attenuation? J. Bacteriol. *185*, 4764–4771.